Available online at www.sciencedirect.com
ScienceDirect
Phytochemistry 68 (2007) 1081–1088
PHYTOCHEMISTRY
www.elsevier.com/locate/phytochem

Oxidative coupling of the pyrogallol B-ring with a galloyl group during enzymatic oxidation of epigallocatechin 3-*O*-gallate

Yan Li, Takashi Tanaka *, Isao Kouno

Graduate School of Biomedical Sciences, Nagasaki University, 1-14 Bunkyo-machi, Nagasaki 852-8521, Japan

Received 12 July 2006; received in revised form 24 October 2006
Available online 22 February 2007

Abstract

In order to clarify the mechanism for formation of catechin oligomers during the fermentation stage of black tea manufacture, epigallocatechin-3-*O*-gallate, the most abundant tea flavanol in fresh tea leaves, was enzymatically oxidized and the resulting unstable quinone metabolites were converted to phenazine derivatives by treatment with *o*-phenylenediamine. In addition to formation of monomeric and dimeric derivatives, four trimeric derivatives were isolated whose structures were determined by application of spectroscopic methods. The derivatives differed from each other in the location of the phenazine moieties and in the atropisomerism of the biphenyl bond. The results suggested that oxidative coupling of the galloyl group with the B-ring proceeds by a quinone dimerization mechanism similar to that for production of theasinensins.

Keywords: *Camellia sinensis*; Theaceae; Black tea; Polyphenol; Oxidation; Epigallocatechin-3-*O*-gallate

1. Introduction

Black tea is the most highly consumed beverage worldwide and amounts to 80% of world tea production (Graham, 1992). Black tea and green tea are made from the same tea plant, *Camellia sinensis*, with the difference between the two depending on when the leaf enzymes were inactivated during manufacturing. In green tea manufacture, the enzymes are inactivated immediately after harvesting of fresh tea leaves, and therefore, the composition of green tea polyphenols, are mainly comprised of (−)-epicatechin, (−)-epigallocatechin and their galloyl esters, similar to those in fresh leaves. On the other hand, in black tea manufacture, the tea catechins are first oxidized with the aid of enzymes, which are then inactivated. The oxidation reactions generate B-ring *o*-quinones of the catechins and cross-coupling reactions of the quinones produce a complex mixture of black tea polyphenols (Haslam, 1998; Tanaka and Kouno, 2003). Although dimeric products, including theaflavins and theasinensins, are known to be important (Hashimoto et al., 1992), the major components of the oxidation products, especially those with an oligomeric nature, so called thearubigins, have yet to be clarified despite assiduous efforts (Haslam, 2003).

To avoid the complexity of cross-coupling reaction in vitro fermentation experiments using pure catechins were very useful for studying catechin oxidation (Sanderson et al., 1972; Robertson, 1983; Guyot et al., 1996; Tanaka et al., 2000a; Tanaka et al., 2002b). We previously examined oxidation of (−)-epigallocatechin-3-*O*-gallate (**1**), the most abundant polyphenol (40–56% of total tea catechins) in tea leaves (Saijo and Takeda, 1999), and succeeded to isolate dehydrotheasinensin A (**2**), an unstable dimer of the quinone of **1** (Scheme 1) (Tanaka et al., 2003). The structure of **2** was apparently an hydrated form of the oxidation products of theasinensins A (**3**) and D (**4**). However, **3** and **4** were not converted to **2** under similar experimental conditions. Therefore, the mechanism for production of **2** was presumed to be electrophilic coupling

* Corresponding author. Tel.: +81 95 819 2433; fax: +81 95 819 2477.
E-mail address: t-tanaka@nagasaki-u.ac.jp (T. Tanaka).

0031-9422/$ - see front matter © 2007 Elsevier Ltd. All rights reserved.
doi:10.1016/j.phytochem.2007.01.005

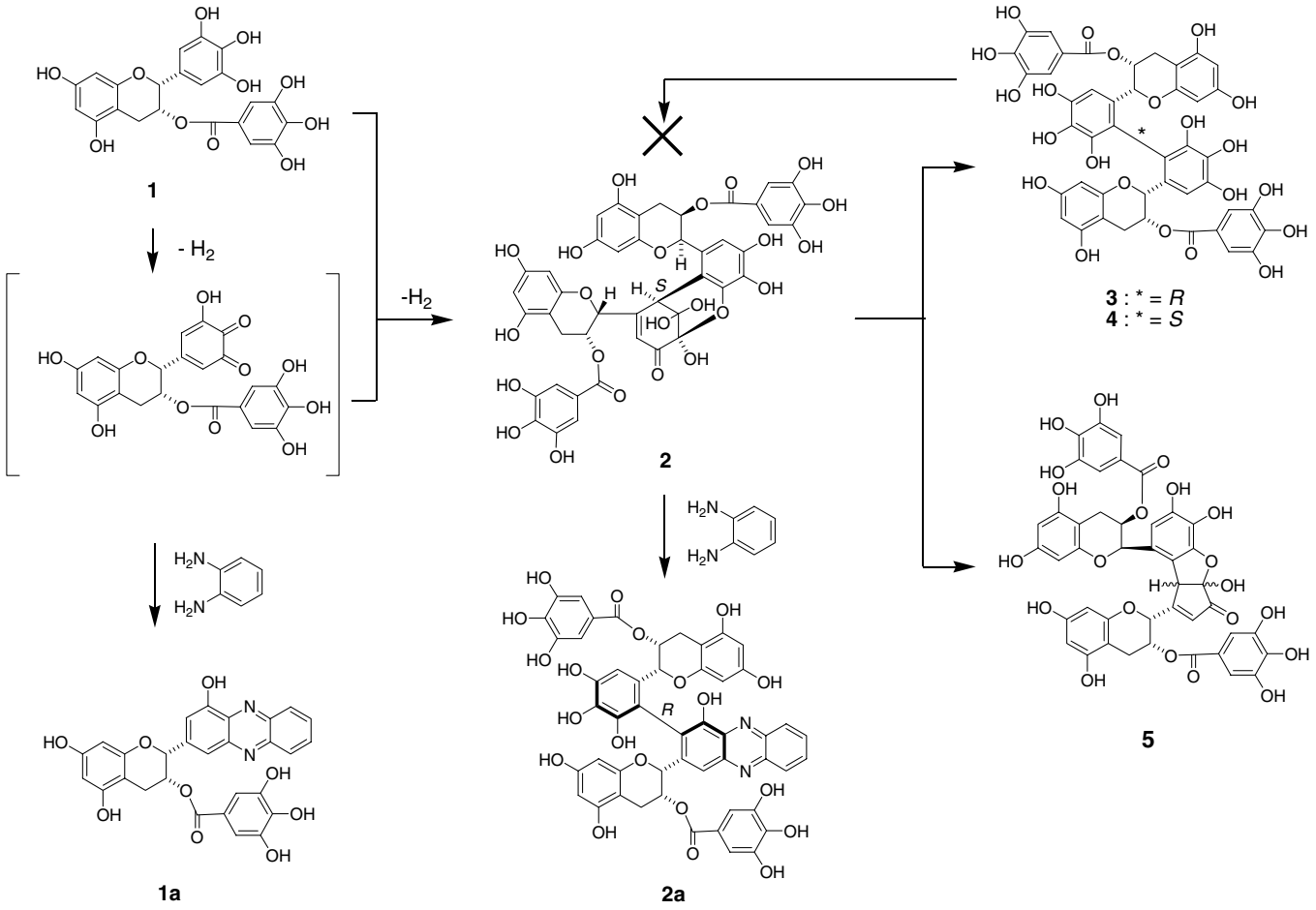

Scheme 1. Proposed formation of coupling products **1**–**5**.

of the quinone **1a** with the pyrogallol B-ring of **1** and subsequent oxidation (Scheme 2). Our previous results also suggested that formation of **2** was highly stereo-selective because reduction of **2** with chemical reagents such as thiol compounds yielded **3** with a *R*-biphenyl bond. In addition, product **2** is a key intermediate in the oxidation of **1** because when decomposed it gives rise to important black tea polyphenols including **3**, **4** and galloyl oolongtheanin (**5**) under mild conditions. The decomposition was presumed to be a redox dismutation, because it afforded the reduction products (**3** and **4**) and the oxidation products (**5** and other minor products). These findings indicate that oxidative coupling between two pyrogallol B-rings is the major oxidation route. More recently, we succeeded in iso-

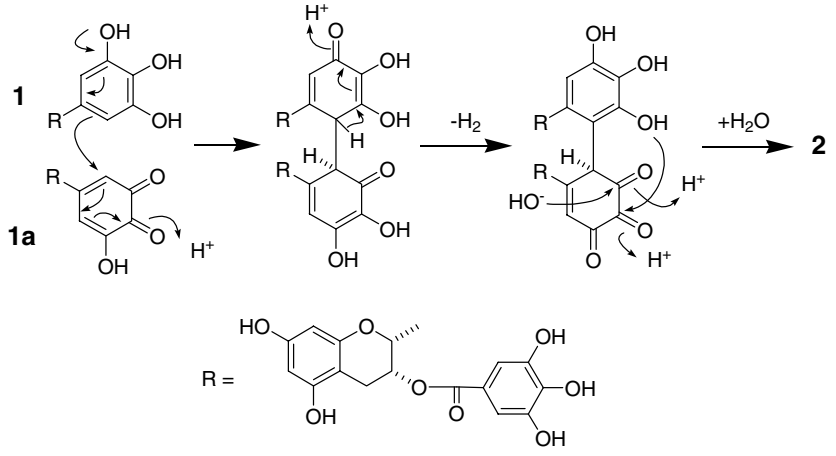

Scheme 2. Proposed mechanism of formation of **2** for **1**/**1a**.

lating a trimer (**6**) from the reaction mixture obtained after chemical reduction of the unstable oxidation products of **1** (Tanaka et al., 2005). The presence of related oxidation products in black tea with further large molecules was also suggested by high performance liquid chromatography-mass spectrometry (HPLC-MS) techniques (Menet et al., 2004). The present study focuses on the production mechanism of catechin oligomers and describes the mechanism for production of trimer **6** and its isomers.

2. Results and discussion

Based on the structural similarity between theasinensins (**3** and**4**) and **6**, we hypothesized that **6** was produced via a trimeric precursor analogous to **2** (Tanaka et al., 2005). However, isolation of the precursor was expected to be difficult because **2** gradually decomposed during chromatographic separation (Tanaka et al., 2003). In addition, the low yield of **6** in the previous study suggested that the concentration of the precursor in the reaction mixture was much lower than that of **2**. Therefore, in the present study, our aim was to isolate the precursor after chemical conversion to its stable derivative. Treatment of **1** with a Japanese pear (a cultivar of *Pyrus pyrifolia*) fruit crude homogenate (Nishimura et al., 2003) afforded a mixture of oxidation products including **2** as the major component. Subsequently, the reaction mixture was treated with an ethanolic solution of *o*-phenylenediamine and acetic acid in order to convert the unstable dehydrotheasinensin analogs to stable phenazine derivatives (Tanaka et al., 2000b, 2002b). Separation of the derivatives was achieved by chromatography over Diaion HP20SS, Sephadex LH-20, Chromatorex ODS, TSK-gel Toyopearl HW40F and preparative HPLC, resulting in four isomers of phenazine derivatives **7a**, **7b**, **8a** and **8b**, of trimeric structure together with monomeric and dimeric phenazine derivatives **1a** and **2a**, respectively (see Scheme 3).

The four phenazine derivatives were obtained as reddish brown amorphous powders and showed characteristic UV absorption at 378 nm, which were similar to that of **2a** indicative of the presence of hydroxyphenazine moieties in the molecules. FABMS exhibited the $[M+H]^+$ peaks at m/z 1511 and the $[M+Na]^+$ peaks at m/z 1533, and the expected molecular weight (1510) was two mass units smaller than the sum of the molecular weights of **1a** and **2a**, indicating that these derivatives have a trimeric structure. This was consistent with the ^1H NMR spectroscopic data listed in Table 1, which showed signals arising from three flavan-3-ol units along with the aromatic resonances due to two phenazine moieties. The ^1H–^1H COSY spectra showed long-range ^1H–^1H couplings between the C-ring H-2 and the adjacent B-ring aromatic protons, and indicated that two of the three B-ring protons resonated at a lower field (in the range of δ 8.1–8.5) compared to usual catechin B-ring protons (δ 6.5–7.1). This observation indicates that two of the three B-rings formed a phenazine moiety in each molecule. A pair of two-proton singlet signals observed around δ 7.0 showed the presence of two galloyl groups, and acylation of three hydroxyl groups at flavan-3-ol C-3 positions was apparent from the low field shifts of the C-ring H-3 signals. This implies that one of the galloyl groups participated in the formation of the interflavan linkage in each trimeric structure.

The HMBC correlations observed for **7a** allowed us to elucidate its structure (Fig. 1). Most of the aromatic carbon signals, except for some overlapping signals attributable to nitrogen- and oxygen-bearing carbons, were assigned based on their long-range correlations with C-ring H-2 signals and aromatic proton signals. The ^3J correlations of ester

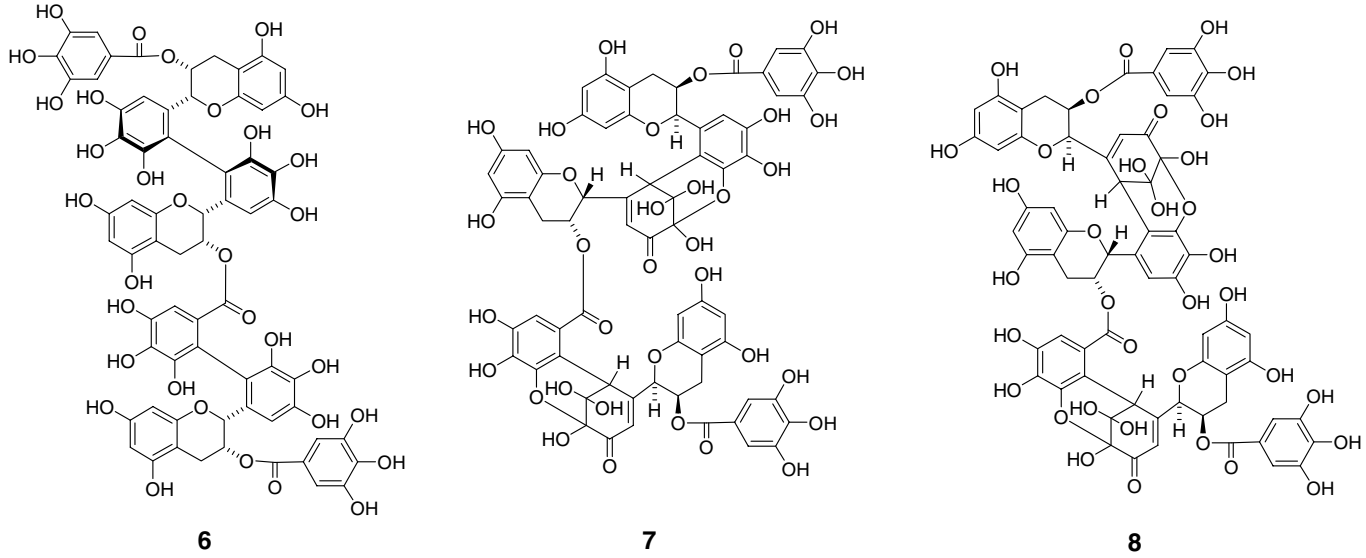

Scheme 3. Structures **6**–**8**.

Table 1
^{1}H NMR spectroscopic data for phenazine derivatives **2a**, **7a**, **7b**, **8a**, and **8b** (in acetone-d_6)

	2a	**7a**	**7b**	**8a**	**8b**
Upper unit					
2	5.19 (*brs*)	4.62 (*s*)	5.07 (*s*)	5.05 (*s*)	5.29 (*s*)
3	5.52 (*brs*)	5.34 (*brs*)	5.76 (*brd*, 2)	5.50 (*brd*, 3)	5.65 (*brd*, 3)
4	3.12 (*d*, 18)	2.69 (*d*, 17)	2.86 (*d*, 17)	2.99 (*d*, 17)	3.05 (*d*, 17)
	2.60 (*dd*, 4, 18)	2.24 (*dd*, 4, 17)	2.54 (*dd*, 4, 17)	2.56 (*dd*, 5, 17)	2.67 (*dd*, 5, 17)
6	6.07[a] (*d*, 2)	5.85 (*d*, 2)	6.39 (*d*, 2)	6.02 (*d*, 2)	6.15 (*d*, 2)
8	5.93[b] (*d*, 2)	5.80 (*d*, 2)	6.26 (*d*, 2)	5.98 (*d*, 2)	6.01 (*d*, 2)
B-6	8.41 (*s*)	7.03 (*s*)	7.13 (*s*)	8.15 (*s*)	8.20 (*s*)
C-3 galloyl-2,6	7.12[c] (2H, *s*)	7.05 (2H, *s*)	7.14 (2H, *s*)	6.96[a] (2H, *s*)	7.08 (2H, *s*)
Middle unit					
2′		4.89 (*s*)	4.92 (*s*)	4.51 (*s*)	4.67 (*s*)
3′		5.39 (*brd*, 5)	5.61 (*brd*, 3)	5.26 (*brs*)	5.21 (*brs*)
4′		2.67 (*d*, 17)	3.06 (*d*, 17)	2.34 (*d*, 17)	2.92 (*d*, 17)
		2.38 (*dd*, 5, 17)	2.68 (*dd*, 5, 17)	2.05 (–[d])	2.30 (*dd*, 4, 17)
6′		5.70 (*d*, 2)	6.17 (*d*, 2)	5.52 (*d*, 2)	6.07 (*d*, 2)
8′		5.49 (*d*, 2)	6.11 (*d*, 2)	5.36 (*d*, 2)	5.93 (*d*, 2)
B′-6		8.20 (*s*)	8.29 (*s*)	7.07 (*s*)	7.16 (*s*)
C-3[1] galloyl-6		7.09 (*s*)	7.11 (*s*)	7.29 (*s*)	7.16 (*s*)
Lower unit					
2″	4.80 (*brs*)	4.89 (*s*)	5.44 (*s*)	5.13 (*s*)	5.30 (*s*)
3″	5.44 (*brs*)	5.24 (*brs*)	5.38 (*brs*)	5.40 (*brd*, 4)	5.24 (*brd*, 3)
4″	2.80 (*d*, 18)	2.86 (*d*, 17)	3.09 (*d*, 17)	2.98 (*d*, 17)	2.90 (*d*, 18)
	2.35 (*dd*, 4, 18)	2.26 (*dd*, 5, 17)	2.54 (*dd*, 4, 17)	2.60 (*dd*, 5, 17)	2.43 (*dd*, 5, 18)
6″	6.06[a] (*d*, 2)	6.15 (*d*, 2)	6.04 (*d*, 2)	6.04 (*d*, 2)	6.22 (*d*, 2)
8″	5.91[b] (*d*, 2)	5.97 (*d*, 2)	5.93 (*d*, 2)	6.26 (*d*, 2)	6.09 (*d*, 2)
B″-6	7.18 (*s*)	8.10 (*d*, 1)	8.47 (*d*, 1)	8.15 (*s*)	8.39 (*s*)
C-3″ galloyl-2,6	7.06[c] (2H, *s*)	6.94 (2H, *s*)	7.16 (2H, *s*)	6.99[a] (2H, *s*)	7.00 (2H, *s*)
Phenazine	7.94 (2H, *m*)	7.85–7.95 (4H, *m*)	7.56 (1H, *brd*, 9)	7.81–7.86 (4H, *m*)	7.71–7.79 (3H, *m*)
	8.27 (2H, *m*)	8.19–8.22 (4H, *m*)	7.61 (1H, *m*)	8.10–8.22 (4H, *m*)	8.19 (1H, *d*, 9)
			7.78 (1H, *m*)		8.25–8.45 (4H, *m*)
			8.03 (2H, *m*)		
			8.17 (1H, *brd*, 9)		
			8.34 (1H, *m*)		
			8.79 (1H, *m*)		

[a,b,c] Assignments may be interchanged.
[d] The signal was overlapped with the solvent signal.

carbonyl carbons with both of the C-ring H-3 and aromatic protons confirmed the location of galloyl esters at the C-3 positions. The ^{13}C-NMR chemical shifts of the B- and B′-rings closely resembled those of **2a**, indicating the presence of the same partial structure. The ^4J correlation between the C-3′ galloyl H-6 and B″-ring C-2 indicated that the C-3′ galloyl group was attached to the B″-ring through a C–C bond. The signals attributable to the C-2 (δ 118.53) and C-3 (δ 149.98) of the B″-ring appeared in the lower and upper field, respectively, compared to the corresponding B′-ring resonances [δ 115.82 (C-2), δ 152.07 (C-3)]. This difference was common to other derivatives (**7b**, **8a**, and **8b**). The HMBC spectrum of **7b** showed correlations similar to those of **7a** and revealed that **7b** and **7a** differs as to whether the attachment at C-2 is R at S, respectively (Fig. 1). On the other hand, **8a** and **8b** were found to be the isomers of **7a** and **7b** based on similar HMBC spectroscopic analysis. In the structures of **7a** and **7b**, the phenazine rings were located at the middle and lower units; whereas the phenazine rings of **8a** and **8b** were located at the upper and lower units as shown in Fig. 1. The results indicate that these four derivatives are isomers in which **1a** is attached to one of the two galloyl groups of **2a**. Previously we have demonstrated that formation of the quinone dimer **2**, and its derivative **2a**, from **1** was highly stereo-selective (Tanaka et al., 2002; Tanaka et al., 2003), and in this experiment **2a** was also isolated as the only dimeric derivative. Therefore, atropisomerism of the biphenyl bond between the upper and middle units of these four trimers was deduced to be in the *R* configuration, implying that each isomer differs only in configuration at the galloyl–phenazine biphenyl bonds.

Despite their 'identical' plane structures, the ^{1}H NMR chemical shifts of **7a** and **7b** were significantly different. Compared to the chemical shifts of the phenazine-bearing catechin unit of **2a**, the A-ring H-6′ and H-8′ and C-ring H-4′ of the middle unit of **7a** resonated at a much higher field (Table 1). Similar up-field shifts were also observed in the spectrum of **8a**; that is, the H-6′, H-8′ and H-4′ of the middle unit appeared at a higher field compared to

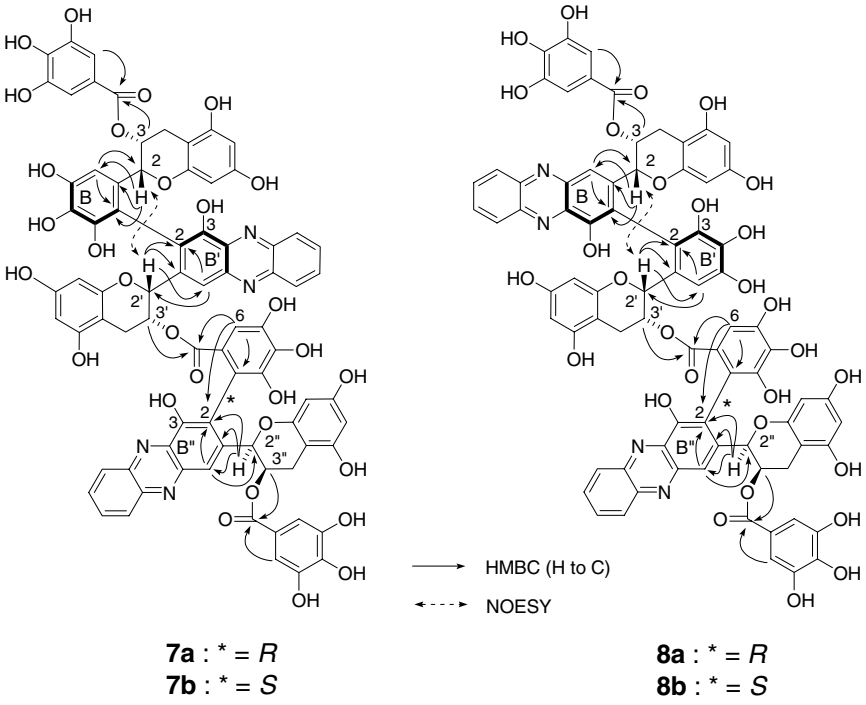

Fig. 1. Important HMBC and NOESY correlations for compounds **7a**, **7b**, **8a**, and **8b**.

the corresponding proton signals of the epigallocatechin unit of **2a**. These up-field shifts of **7a** and **8a** were deduced to be caused by shielding effects of phenazine ring of the lower units. This shielding effect was not observed in the spectra of **7b** and **8b**. This difference strongly supports the suggestion that **7a** and **8a** are atropisomers of **7b** and **8b**, respectively, at the galloyl-phenazine bonds. An attempt to determine the total stereochemistry of the four derivatives by NOESY spectroscopic analysis failed. The spectra of all derivatives showed strong NOEs between H-2 of the upper unit and H-2′ of the middle unit; however, no clear information was obtained about conformation between the middle and lower units. Molecular modeling of the isomer with a *R*-biphenyl bond between the galloyl and B″-ring with the aid of CS MOPAC® suggested that the A- and C-rings of the lower unit are oriented on the opposite side of the middle unit when the phenazine unit of the lower unit is located directly underneath the A- and C-rings of the middle unit (Fig. 2). In contrast, in the isomer with a *S*-biphenyl bond, the A- and C-rings of

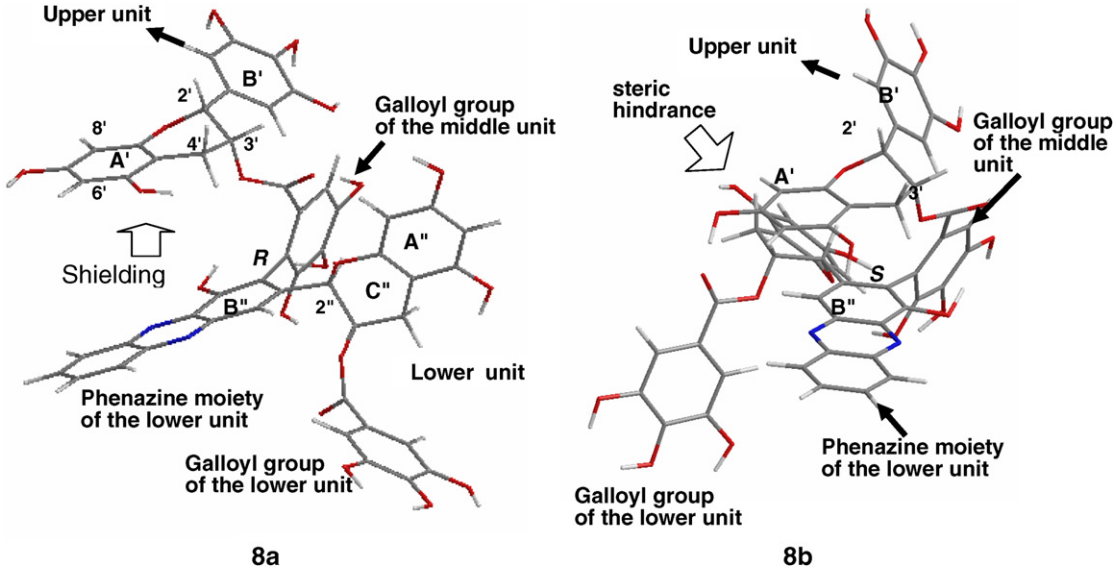

Fig. 2. Partial stereo structures of **8a** and **8b**.

the lower and middle units were oriented on the same side when the phenazine unit shielded the middle unit, and thus, the conformation was suggested to be less stable due to steric hindrance between the two sets of flavan A- and C-rings. Therefore, atropisomerism of the galloyl and B-ring pyrogallol rings was presumed to be *R* configuration in **7a** and **8a**, the middle units of which were strongly shielded by a phenazine unit.

3. Concluding remarks

Formation of the four derivatives **7a**, **7b**, **8a** and **8b** in this study revealed that dehydrotheasinensin-type trimeric intermediates **7** and **8** were produced in the reaction mixture. These findings also strongly suggest that formation of a biphenyl bond between galloyl group and pyrogallol-type B-ring in the production of trimer **6** proceeded by a mechanism similar to formation of theasinensins (Scheme 1). In the present experiment, dimeric derivatives having a galloyl–B-ring biphenyl bond were not obtained. It was presumed that the coupling between two B-rings occurred predominantly to yield **2** due to the lower reactivity of galloyl groups, and subsequently oxidation of the galloyl groups of **2** occurred to yield the trimeric derivatives **7** and **8**. Since decomposition of **2** afforded theasinensin A (**3**) and D (**4**), oolongtheanin (**5**) and other minor products (Tanaka et al., 2003), numerous products besides **6** were expected to be produced via **7** and **8**. Furthermore, tetramers and oligomers of **1** were also possibly produced by an analogous mechanism. The mechanism proposed here may be important in the formation of complex black tea polyphenols, because a major component of tea catechins in fresh tea leaves is galloylated.

4. Experimental

4.1. General

Optical rotations were measured with a JASCO DIP-370 digital polarimeter whereas CD spectra were measured with JASCO J-720w apparatus. ^{1}H and ^{13}C NMR, ^{1}H–^{1}H COSY, NOESY, HSQC and HMBC spectra were recorded using a Unity *plus* 500 spectrometer (Varian Inc, USA) operating at 500 MHz for ^{1}H and 125 MHz for ^{13}C. ^{1}H and ^{13}C NMR spectra were also measured with a JEOL JMN-AL400 (JEOL Ltd., Japan) operating at 400 MHz for ^{1}H and 100 MHz for ^{13}C. FAB and EIMS were recorded on a JMS DX-303 spectrometer (JEOL Ltd.), and *m*-nitrobenzyl alcohol or glycerol was used as the matrix for FABMS. Elemental analysis was conducted with a PerkinElmer 2400 II analyzer (PerkinElmer, Inc.). CC was conducted on MCI-gel CHP 20P (Mitsubishi Chemical Co.), Chromatorex ODS (Fuji Silysia Chemical Ltd., Japan), and Sephadex LH-20 (Pharmacia Fine Chemical Co.). TLC was performed on 0.2 mm thick precoated Kieselgel 60 F_{254} plates (Merck) with benzene-ethyl formate-formic acid (1:7:1, v/v) or $CHCl_3$–MeOH–H_2O (14:6:1, v/v) and spots were detected by UV illumination, sprayed with 2% ethanolic $FeCl_3$ or 10% sulfuric acid reagent, and heated. Analytical HPLC was performed on a Cosmosil 5C_{18}-AR II column (Nacalai Tesque Inc.; 250 × 4.6 mm i.d.) with gradient elution from 10%–30% (30 min) and 30%–75% (15 min) of MeCN in 50 mM H_3PO_4 (flow rate, 0.8 mL/min; detection: JASCO photodiode array detector MD-910). Preparative HPLC was performed on a COSMOSIL 5C_{18}-AR-II column (Nacalai Tesque Inc.; 10 mm i.d. × 250 mm) with 20%–70% MeCN in 0.5% TFA (a linear gradient elution). Epigallocatechin was isolated from commercial green tea and recrystallized from H_2O.

4.2. Oxidation, derivatization and separation

Fresh Japanese pear (1.5 kg) was homogenized with H_2O (500 ml) in a Waring blender and filtered through four layers of gauze. The homogenate was mixed with an aqueous solution (500 ml) of **1** (10 g) and vigorously stirred for 120 min at room temperature. The mixture was poured into a 1% solution of *o*-phenylenediamine in 10% AcOH–EtOH (3 l) and stirred for 2 h at room temperature. After filtration, the filtrate was concentrated (to ~800 ml) and subjected to Diaion HP20SS (6 cm i.d. × 20 cm) CC eluted 10% stepwise with 10%–100% MeOH in H_2O to give eight fractions: frs 1 (0.12 g), 2 (0.54 g), 3 (2.35 g), 4 (1.93 g), 5 (0.81 g), 6 (1.13 g), 7 (0.44 g) and 8 (0.98 g). Fractions 2–4 mainly contained **1** and the EGCg quinone dimer (Valcic et al., 1999; Tanaka et al., 2003). Fractions 5 and 8 contained pure products and were identified as **2a** and **1a** by comparison of ^{1}H NMR spectroscopic data and co-HPLC. Fraction 6 was further separated into three fractions (frs 6-1 – 6-3) by Sephadex LH-20 chromatography (3.5 cm i.d. × 25 cm) with H_2O–MeOH (10% stepwise elution of 30%–100%). Fraction 6-3 (158 mg) was applied to a column of Chromatorex ODS (3 cm × 15 cm) with 30%–100% MeOH to give **8b** (60.5 mg). Fraction 6-1 (246 mg) was successively subjected to Chromatorex ODS (3 cm × 15 cm, 5% stepwise elution of 30%–100% MeOH) and Toyopearl HW-40 F (3 cm × 25 cm, 10% stepwise elution of 30%–100% MeOH) chromatographic purification and finally purified by preparative HPLC to give **8a** (38 mg) and **7a** (19 mg). Similar chromatographic separation of fr. 7 yielded **7b** (10 mg).

4.2.1. Phenazine derivative *7a*

Reddish brown amorphous powder; $[\alpha]_D^{28}$ −380.6 (*c* 0.05, MeOH); FABMS *m/z* 1511 $[M+H]^+$, 1533 $[M+Na]^+$; UV (EtOH) λ_{max} nm (logε): 271 (5.09), 378 (4.14); IR ν_{max} cm^{-1}: 3389, 1694, 1613, 1516, 1467; For ^{1}H NMR (500 MHz, acetone-d_6) spectrum see Table 1;^{13}C NMR (125 MHz, acetone-d_6) δ: 166.99 (C-3′ galloyl C-7), 166.30 (C-3″ galloyl-7), 166.04 (C-3 galloyl-7), 157.60, 157.34, 157.11(3C), 157.00, 156.84(2C), 156.53 (A-ring C-5, 7, 8a), 152.07 (B′-3), 149.98 (B″-3), 146.49 (B-5),

145.79(4C) (C-3, 3″ galloyl-3,5), 145.57 (C-3′ galloyl-5), 144.80 (B′-5), 144.33 (B″-1), 143.90 (B-3), 143.14 (B′-1), 144.69, 143.42, 142.41, 142.22, 142.18(2C) (B-7,8, B″-5,7,8, C-3′ galloyl-3), 138.89 (C-3′ galloyl-4), 138.78, 138.46 (C-3′,3″ galloyl-4), 135.78 (B″-4), 135.37 (B′-4), 134.02 (B-4), 131.90, 131.80, 131.45, 130.99, 130.21(3C), 129.36 (phenazine), 128.23 (B-1), 121.91 (C-3″ galloyl-1), 121.41 (C-3 galloyl-1), 120.47 (C-3′ galloyl-1), 119.44 (B′-6), 118.53 (B″-2), 117.84 (B″-6), 115.82 (B′-2), 115.73 (C-3′ galloyl-2), 112.20 (B-2), 111.98 (C-3′ galloyl-6), 109.91 (C-3 galloyl-2,6), 109.69 (C-3″ galloyl-2,6), 108.63 (B-6), 98.70 (C-4a′), 98.52 (C-4a), 98.30 (C-4a″), 96.66 (C-6′), 96.65 (C-8″), 96.34 (C-6), 96.11 (C-6″), 95.76 (C-8), 95.54 (C-8′), 76.48 (C-2″), 76.39 (C-2′), 76.18 (C-2), 68.50 (C-3), 68.41 (C-3′), 67.63 (C-3″), 26.92, 26.61, 26.53 (C-4,4′,4″). (Found: C, 55.78; H, 4.09; N, 3.38. $C_{78}H_{54}N_4O_{29}$ $9H_2O$ requires: C, 55.99; H, 4.34; N, 3.35.)

4.2.2. Phenazine derivative *7b*

Reddish brown amorphous powder; $[\alpha]_D^{29}$ −116.7 (*c* 0.05, MeOH); FABMS *m/z* 1511 $[M+H]^+$, 1533 $[M+Na]^+$; UV (EtOH) λ_{max} nm (log ε): 271 (5.05), 378 (4.12); IR ν_{max} cm^{-1}: 3389, 1697, 1632, 1517, 1467; For ^1H NMR (500 MHz, acetone-d_6) spectra, see Table 1; ^{13}C NMR (125 MHz, acetone-d_6) δ: 166.43 (C-3′ galloyl C-7), 166.34 (C-3 galloyl-7), 166.22 (C-3″ galloyl-7), 157.73, 157.60, 157.55, 157.41, 157.29, 157.24, 157.16, 157.06(2C) (A-ring C-5, 7, 8a), 151.83 (B′-3), 150.05 (B″-3), 145.88 (B-5), 145.78(2C), 145.74(2C) (C-3, 3″ galloyl-3,5), 145.15 (C-3′ galloyl-5), 144.19(2C), 143.97, 143.64, 143.39, 142.76, 142.21 (B-7,8, B′-5, B″-5,7,8, C-3′ galloyl-3), 144.19 (B″-1), 143.22 (B-3), 142.85 (B′-1), 138.49 (C-3 galloyl-4), 138.46 (C-3″ galloyl-4), 138.12 (C-3′ galloyl-4), 135.64 (B′-4), 135.85 (B″-4), 132.97 (B-4), 132.04, 131.76, 131.43, 130.79, 130.62, 130.56, 129.72, 129.64 (phenazine), 130.36 (B′-1), 123.61 (C-3′ galloyl-1), 122.24 (C-3 galloyl-1), 122.10 (C-3″ galloyl-1), 120.30 (B″-2), 119.26 (B′-2), 119.20 (B′-6), 118.02 (B″-6), 116.49 (C-3′ galloyl-2), 112.88 (B-2), 111.20 (C-3′ galloyl-6), 109.96 (C-3 galloyl-2,6), 109.77 (C-3″ galloyl-2,6), 108.47 (B-6), 99.12 (C-4a′), 98.96 (C-4a), 98.85 (C-4a″), 97.30 (C-6), 97.16 (C-6′), 96.89 (C-8), 96.30 (C-6″), 96.17 (C-8″), 95.95 (C-8′), 77.27 (C-2″), 76.70 (C-2), 75.64 (C-2′), 68.24 (C-3), 67.85 (C-3″), 67.14 (C-3′), 28.21, 26.86(2C) (C-4,4′,4″). (Found: C, 55.71; H, 4.29; N, 3.02. $C_{78}H_{54}N_4O_{29}$ $9H_2O$ requires: C, 55.99; H, 4.34; N, 3.35.)

4.2.3. Phenazine derivative *8a*

Reddish brown amorphous powder; $[\alpha]_D^{29}$ −268.6 (*c* 0.06, MeOH); FABMS *m/z* 1511 $[M+H]^+$, 1533 $[M+Na]^+$; UV (EtOH) λ_{max} nm (log ε): 272 (5.10), 378 (4.16); IR ν_{max} cm^{-1}: 3389, 1697, 1632, 1517, 1467; For ^1H NMR (500 MHz, acetone-d_6) spectrum, see Table 1;^{13}C NMR (125 MHz, acetone-d_6) δ: 166.70 (C-3′ galloyl C-7), 166.41, 165.23 (C-3, 3″ galloyl-7), 157.61(3C), 157.30, 157.20, 156.97, 156.86, 156.58(2C) (A-ring C-5, 7, 8a), 151.93 (B-3), 149.95 (B″-3), 146.64 (B′-5), 145.79(4C)(C-3, 3″ galloyl-3,5), 145.60 (C-3′ galloyl-5), 144.65(2C), 144.57(2C), 144.54(2C), 143.82, 142.37, 142.11 (B-5,7,8, B′-3, B″-1,5,7,8, C-3′ galloyl-3), 142.75 (B-1), 138.75(2C) (C-3,3″ galloyl-4), 138.36 (C-3′ galloyl-4), 135.64, 135.60 (B-4, B″-4), 133.78 (B′-4), 131.80(2C), 131.30, 131.01, 130.25, 130.02, 129.94, 129.39 (phenazine), 128.74 (B′-1), 121.87 (C-3′ galloyl-1), 121.49, 121.39 (C-3, 3″ galloyl-1), 119.49 (B-6), 118.71 (B″-2), 117.93 (B″-6), 116.66 (B-2), 115.49 (C-3′ galloyl-2), 111.96 (C-3′ galloyl-6), 111.44 (B′-2), 109.74 (C-3,3″ galloyl-2,6), 108.41 (B′-6), 98.68 (C-4a′), 98.56 (C-4a″), 98.51 (C-4a), 96.71(2C) (C-6,6″), 96.38 (C-8″), 96.30 (C-6′), 95.92 (C-8), 95.33 (C-8′), 76.47(2C) (C-2, 2″), 76.10 (C-2′), 68.24 (C-3′), 67.95, 67.68 (C-3, 3″), 27.04, 26.97 (C-4′, 4″), 26.45 (C-4). (Found: C, 55.10; H, 4.05; N, 3.37. $C_{78}H_{54}N_4O_{29}$ $10H_2O$ requires: C, 55.39; H, 4.41; N, 3.31.)

4.2.4. Phenazine derivative *8b*

Reddish brown amorphous powder; $[\alpha]_D^{29}$ −540.0 (*c* 0.06, MeOH); FABMS *m/z* 1511 $[M+H]^+$, 1533 $[M+Na]^+$; UV (EtOH) λ_{max} nm (log ε): 272 (5.36), 378 (4.17); IR ν_{max} cm^{-1}: 3390, 1695, 1613, 1515, 1465; For ^1H NMR (500 MHz, acetone-d_6) spectrum, see Table 1; ^{13}C NMR (125 MHz, acetone-d_6) δ: 166.47 (C-3″ galloyl C-7), 166.37 (C-3 galloyl-7), 165.88 (C-3′ galloyl-7), 157.82, 157.75, 157.51, 157.47, 157.44(2C), 157.28, 157.21, 157.12 (A-ring C-5, 7, 8a), 151.54 (B-3), 149.83 (B″-3), 146.31 (B′-5), 145.82(4C)(C-3, 3″ galloyl-3,5), 145.34 (C-3′ galloyl-5), 144.58, 144.43, 144.20, 144.12, 143.91, 143.76, 143.66, 143.58, 142.17, 141.95 (B-1,5,7,8, B′-3, B″-1,5,7,8, C-3′ galloyl-3), 138.74 (C-3″ galloyl-4), 138.70 (C-3 galloyl-4), 138.32 (C-3′ galloyl-4), 135.66 (B″-4), 135.38 (B-4), 134.21 (B′-4), 131.62, 131.50, 131.11, 130.98, 130.47, 129.99, 129.93, 129.87 (phenazine), 128.20 (B′-1), 123.24 (C-3′ galloyl-1), 121.76 (C-3 galloyl-1), 121.45 (C-3″ galloyl-1), 119.71 (B″-2), 119.11 (B-6), 118.25 (B″-6), 116.91 (B-2), 116.36 (C-3′ galloyl-2), 113.84 (B′-2), 111.64 (C-3′ galloyl-6), 109.91 (C-3 galloyl-2,6), 109.80 (C-3″ galloyl-2,6), 109.11 (B′-6), 99.22 (C-4a′), 98.85 (C-4a), 98.75 (C-4a″), 97.29 (C-8′), 96.87 (C-8″), 96.59 (C-8′), 96.58 (C-6′), 96.28 (C-6″), 95.94 (C-6), 77.06 (C-2″), 76.66 (C-2), 76.20 (C-2′), 68.20 (C-3′), 67.93(2C) (C-3, 3″), 27.22, 27.12, 26.97 (C-4, 4′, 4″). (Found: C, 55.91; H, 4.15; N, 3.10. $C_{78}H_{54}N_4O_{29}$ $9H_2O$ requires: C, 55.99; H, 4.34; N, 3.35.)

Acknowledgments

The authors are also grateful to Mr. K. Inada, Mr. N. Yamaguchi and Mr. M. Owatari (Nagasaki University) for NMR and MS measurements and elemental analyses.

References

Graham, H.N., 1992. Green tea composition, consumption, and polyphenol chemistry. Preventive Med. 21, 334–350.

Guyot, S., Vercauteren, J., Cheynier, V., 1996. Structural determination of colorless and yellow dimers resulting from (+)-catechin coupling catalyzed by grape polyphenoloxidase. Phytochemistry 42, 1279–1288.

Hashimoto, F., Nonaka, G., Nishioka, I., 1992. Tannins and related compounds. CXIV. Structures of novel fermentation products, theogallinin, theaflavonin and desgalloyl theaflavonin from black tea, and changes of tea leaf polyphenols during fermentation. Chem. Pharm. Bull. 40, 1383–1389.

Haslam, E., 1998. Quinone tannin and oxidative polymerization. In: Haslam, E. (Ed.), Practical polyphenolics from Structure to Molecular Recognition and Physiological Action. Cambridge University Press, Cambridge, pp. 335–373.

Haslam, E., 2003. Thoughts on thearubigins. Phytochemistry 64, 61–73.

Menet, M.C., Sang, S., Yang, C.S., Ho, C.T., Rosen, R.T., 2004. Analysis of theaflavins and thearubigins from black tea extract by MALDI-TOF mass spectrometry. J. Agric. Food Chem. 52, 2455–2461.

Nishimura, M., Fukuda, C., Murata, M., Homma, S., 2003. Cloning and some properties of Japanese pear (*Pyrus pyrifolia*) polyphenol oxidase, and changes in browning potential during fruit maturation. J. Sci. Food Agric. 83, 1156–1162.

Robertson, A., 1983. Effects of catechin concentration on the formation of black tea polyphenols during in vitro oxidation. Phytochemistry 22, 897–903.

Saijo, R., Takeda, Y., 1999. HPLC analysis of catechins in various kinds of green teas produced in Japan and abroad. Nippon Shokuhin Kagaku Kogaku Kaishi 46, 138–147 (CAN 130:351456).

Sanderson, G.W., Berkowitz, J.E., Co, H., Graham, H.N., 1972. Biochemistry of tea fermentation. Products of the oxidation of tea flavanols in a model tea fermentation system. J. Food Sci. 37, 399–404.

Tanaka, T., Betsumiya, Y., Mine, C., Kouno, I., 2000a. Theanaphthoquinone, a novel pigment oxidatively derived from theaflavin during tea-fermentation. Chem. Commun., 1365–1366.

Tanaka, T., Kondou, K., Kouno, I., 2000b. Oxidation and epimerization of epigallocatechin in banana fruits. Phytochemistry 53, 311–316.

Tanaka, T., Mine, C., Inoue, K., Matsuda, M., Kouno, I., 2002a. Synthesis of theaflavin from epicatechin and epigallocatechin by plant homogenates and role of epicatechin quinone in the synthesis and degradation of theaflavin. J. Agric. Food Chem. 50, 2142–2148.

Tanaka, T., Mine, C., Watarumi, S., Fujioka, T., Mihashi, K., Zhang, Y.J., Kouno, I., 2002b. Accumulation of epigallocatechin quinone dimers during tea fermentation and formation of theasinensins. J. Nat. Prod. 65, 1582–1587.

Tanaka, T., Watarumi, S., Matsuo, Y., Kamei, M., Kouno, I., 2003. Production of theasinensins A and D, epigallocatechin gallate dimers of black tea, by oxidation-reduction dismutation of dehydrotheasinensin A. Tetrahedron 59, 7939–7947.

Tanaka, T., Kouno, I., 2003. Oxidation of tea catechins: chemical structures and reaction mechanism. Food Sci. Technol. Res. 9, 128–133.

Tanaka, T., Matsuo, Y., Kouno, I., 2005. A novel black tea pigment and two new oxidation products of epigallocatechin-3-*O*-gallate. J. Agric. Food Chem. 53, 7571–7578.

Valcic, A., Muders, A., Jacobsen, N.E., Liebler, D.C., Timmermann, B.N., 1999. Antioxidant chemistry of green tea catechins. Identification of products of the reaction of (−)-epigallocatechin gallate with peroxyl radicals. Chem. Res. Toxicol. 12, 382–386.